High Temperatures-High Pressures, Vol. 52, pp. 341–350
Reprints available directly from the publisher
Photocopying permitted by license only
DOI: 10.32908/hthp.v52.1375

Determining the density of molten Y_2O_3 using an electrostatic levitation furnace in the International Space Station

Hirohisa Oda*, Rina Shimonishi, Chihiro Koyama,
Tsuyoshi Ito and Takehiko Ishikawa

Japan Aerospace Exploration Agency (JAXA), 2-1-1 Sengen, Tsukuba, Ibaraki 305-8505, Japan

Received: November 6, 2022; Accepted: January 13, 2023.

This work employed the electrostatic levitation furnace (ELF) apparatus installed in the KIBO Japanese Experiment Module on the International Space Station. The ELF is able to levitate high-melting-point materials such as ceramics without containers. The heating and melting of refractory oxides in this apparatus allows the analysis of various thermophysical properties, including density, surface tension and viscosity, that are otherwise very difficult to measure in terrestrial laboratories. In the present study, the density of molten Y_2O_3 was determined over a wide temperature range using the ELF. A density of 4700 kg/m^3 was obtained at 2712 K, in good agreement with the value previously obtained using an aero-acoustic levitator. The relationship between the ionic radius and the molar volume of liquid Y_2O_3 was ascertained and found to be similar to those for other non-glass-forming sesquioxides.

Keywords: density, Y_2O_3, electrostatic levitation furnace, International Space Station, ionic radius

1 INTRODUCTION

As additive manufacturing technologies involving ceramic materials, such as three-dimensional printing, have progressed [1], it has become necessary to ascertain the thermophysical properties of various molten oxides [2]. However, due to the high melting points of these compounds and the risk of

*Corresponding author: oda.hirohisa@jaxa.jp

contamination from containers, the use of conventional techniques and apparatus such as crucibles has become challenging. Many materials may also react with containers at high temperatures, or the container may melt before the sample does. An alternative is to use a levitation furnace to process the sample, which permits melting and solidification without a container. There are three types of levitation furnaces: aerodynamic (ADL) [3, 4], electromagnetic (EML) [5, 6, 7, 8] and electrostatic [9]. The ADL furnace levitates the sample with a gas jet and so the gas flow itself can affect the molten material. In contrast, an EML furnace levitates the sample using the Lorentz force, such that only conductive materials can be processed. In the case of an electrostatic levitation furnace, the sample is levitated via the Coulomb force between the material and electrodes. This type of furnace has the advantage of being able to process insulators such as ceramics.

The Electrostatic Levitation Furnace for the International Space Station (ISS-ELF) developed by the Japan Aerospace Exploration Agency (JAXA) was installed in the KIBO Japanese Experiment Module on the ISS in 2015 (Figure 1) [10, 11]. Since that time, this apparatus has been used to determine the thermophysical properties of refractory oxides that are otherwise exceedingly difficult to measure by conventional methods. Table 1 summarizes the thermophysical properties of various oxides as obtained using the ISS-ELF. These sesquioxides are known not to form glasses. Our group has therefore investigated the atomic structures and thermophysical properties of these compounds in their liquidus phases to establish the factors that determine whether or not an oxide will have a glass phase. The present paper reports the determination of the density of molten Y_2O_3. This oxide has potential applications in ceramics and glasses because it has a high melting point and imparts shock resistance and low thermal expansion characteristics [12].

FIGURE 1
The KIBO ELF on the ISS.

TABLE 1
Thermophysical properties of molten oxides as determined using the ISS-ELF

Oxides	T_m (K)	Thermophysical properties assessed	References
Al_2O_3	2345	Density, surface tension, viscosity	[11, 13]
Tb_2O_3	2683	Density, surface tension, viscosity	[14, 15]
Gd_2O_3	2693	Density	[14]
Ho_2O_3	2685	Density	[14]
Er_2O_3	2686	Density	[14]
Tm_2O_3	2698	Density	[15]
Yb_2O_3	2708	Density	[15]
Lu_2O_3	2763	Density	[15]
Y_2O_3	2712	Density	This work

2 EXPERIMENTAL METHODS

2.1 Electrostatic levitation furnace

A detailed description of the ELF can be found in our earlier papers [11, 13]. Figure 2 shows the ELF chamber while Figure 3 presents a diagram of the position control system associated with this apparatus and Table 2 summarizes the ELF specifications. The position of the sample in this apparatus is controlled using three pairs of electrodes, with a voltage up to 3 kV applied between each pair. The sample is illuminated and the shadow of the specimen is captured by two charge coupled device cameras as a means of monitoring its position. The resulting position information is sent to the ELF controller which then adjusts the voltages applied to the electrodes to modify the sample position. The sample is heated by four semiconductor lasers (each operating

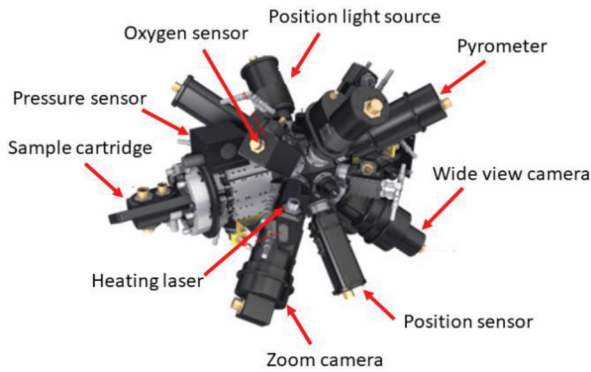

FIGURE 2
The ELF chamber.

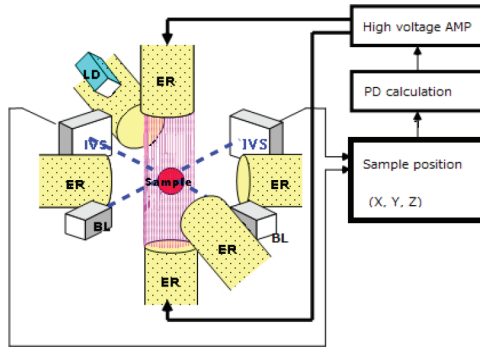

FIGURE 3
Diagram of ELF position control system.

(ER; Electrode, IVS; Intelligent Vision System, BL; Back Light, LD; Laser Diode)

TABLE 2
ELF specifications

Parameter	Value
Size	590 × 887 × 787 mm
Mass	245 kg
Power consumption	550 W
Sample types	Oxide, insulator, metal, alloy
Sample size	2 mm diameter
Atmosphere	Argon, air (max. 2 atm)
Heating source	Four semiconductor lasers (980 nm, max 40 W)
Temperature range	299–3000 °C

at 980 nm and 40 W) installed in a tetrahedral formation. The laser power can be controlled remotely from the ground. The sample temperature is measured using a single-color pyrometer that captures the intensity of radiation over the wavelength range of 1.45 to 1.8 μm.

2.2 Density measurement

The density of molten materials can be determined using the ELF by first levitating the sample at the center of the chamber and subsequently heating it with the lasers. After the sample melts, the lasers are turned off and, as the material cools, its temperature decreases to a supercooled temperature, increases to its melting point (that is, recalescence occurs) and then decreases as the sample solidifies at room temperature. A black and white camera with a non-telecentric zoom lens is used to capture magnified video images of the

specimen with ultraviolet (UV) backlighting at a frequency of 60 Hz. A typical image is presented in Figure 4. Because the molten sample adopts a spherical morphology in the microgravity environment onboard the ISS, the volume of the material can readily be calculated from these images. The perimeter of the sample is determined by computer-based image analysis, which requires a suitable degree of contrast between the sample and the background. At high temperatures, the specimen generates significant infrared radiation that blurs the contours of the sphere and can lead to overestimation of the sample volume. This effect is avoided by acquiring images at a wavelength of approximately 380 nm, where the sample radiation output is less pronounced.

As noted, each sample volume in the present work was calculated using computer-based image analysis [16]. Using still images extracted from the video, 400 edge points around the specimen were identified and converted to polar coordinates (R, θ). These points were subsequently fitted using a fifth order spherical harmonic function:

$$R(\theta) = \sum_{n=0}^{5} c_n P_n(\cos\theta),$$

where $P_n(\cos\theta)$ is an n$^{\text{th}}$ order Legendre polynomial and c_n is a coefficient chosen to minimize the value given by the function.

$$\mathrm{F} = \sum_{j=1}^{400} \{R_j - R_j(\theta)\}^2.$$

Following this, the volume was calculated using the equation

$$V = \frac{2\pi}{3} \int_0^{\pi} R^3(\theta) \sin\theta d\theta.$$

The sample was weighed after its return to Earth to find its mass (m) and the destiny was then calculated as

$$\rho = \frac{m}{V}.$$

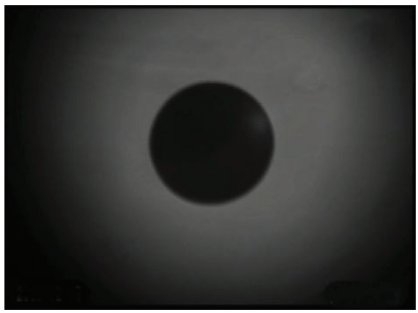

FIGURE 4
Magnified image of UV-backlit Y_2O_3 sample.

3 RESULTS AND DISCUSSION

This work employed Y_2O_3 powder (Nilaco, Y-837050, purity = 99.999 wt%, particle diameter = 2 μm). Spherical samples each having a 2 mm diameter were prepared from this powder using a ground-based aerodynamic levitator and these samples were subsequently processed in the ELF chamber under dry air at a pressure of 2 atm. Figure 5 shows a typical sample temperature profile. The levitated sample was melted successfully and the emissivity of molten sample was used to ascertain its temperature via the pyrometer. It should be noted that the emissivity of the oxide was required to determine its temperature from the pyrometer readings. Unfortunately, the emissivity of molten Y_2O_3 is unknown and so sample temperatures were calculated assuming an emissivity of 1.0 and then adjusted after the experimental work so that the observed temperature plateau matched the melting point of Y_2O_3 (2712 K) [17], assuming that the emissivity of liquid Y_2O_3 was constant. The data indicated that the Y_2O_3 underwent shallow undercooling.

While in the liquidus phase, the sample remained spherical. The aspect ratio (the ratio between the vertical and horizontal diameters) determined for specimen from the image analysis data was in the range of 1.0 ± 0.003. After melting and cooling, the sample showed slight mass losses due to evaporation during the experiment. In case of this report, a sample whose initial mass was 10.28 mg was examined to calculate density. Its mass has been reduced to

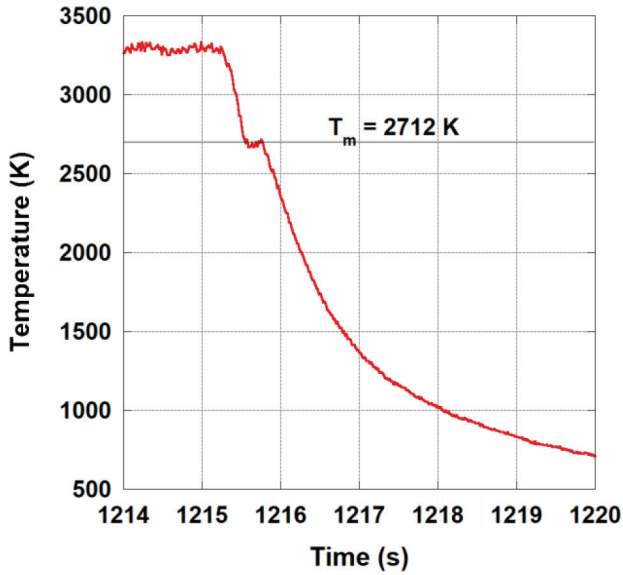

FIGURE 5
temperature profile (time-temperature curve) for a molten Y_2O_3 sample during rapid cooling.

10.23 mg after the experiment, and the density was calculated over a wide temperature range from 2670 to 3300 K using the final mass (10.23 mg).

Figure 6 plots the measured density of the molten Y_2O_3 as a function of temperature. The density of molten Y_2O_3 was found to be 4700 kg/m^3 at its melting point of 2712 K, and the density data also exhibit an inverse linear correlation with temperature. This relationship can be expressed at a confidence interval of 95% as:

$$\rho(T) = (4670 \pm 73) - (0.25 \pm 0.02)(T - T_m).$$

The densities of molten Y_2O_3 obtained from the literature are also plotted in Figure 6 for comparison purposes. Granier and Heurnault measured the density of molten Y_2O_3 using an ADL furnace [18] and obtained a value of 4400 kg/m^3 at the melting point, which was 7% lower than our value. Ushakov et al. determined the density of molten Y_2O_3 using an aero-acoustic levitator (AAL) [2] and their reported value of 4600 kg/m^3 at the melting temperature agrees with the present value within the experimental uncertainty. As discussed by Ushakov et al., the sample was observed from overhead in the work by Grainer and the volume was calculated assuming a spherical specimen. However, a sample levitated by a gas jet will not be a perfect sphere but rather an oblate spheroid. Moreover, Grainer determined the sample outline based on the self-luminosity of the material. These factors would cause the sample volume to be overestimated such that the density would be underestimated.

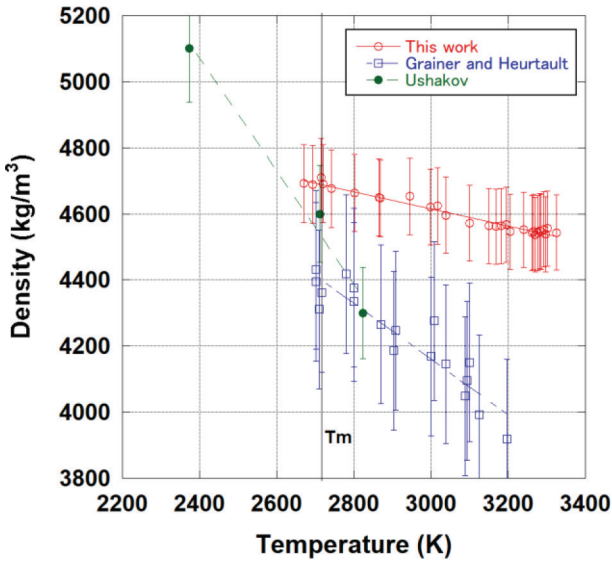

FIGURE 6
Densities of molten Y_2O_3 as functions of temperature. The magnitude of error bars are respectively 2.5% for this work, 3.5% for Granier and Heurtault [18], and 3.2% for Ushakov [2].

The temperature dependence of density obtained using the AAL furnace was much greater than that obtained in the present research. The densities and temperatures measured by Ushakov with the AAL method also fluctuated substantially. This fluctuation has been attributed to non-symmetrical oscillation of the molten sample in the acoustic field [2].

During analyses with the ELF on the ISS, the sample position was maintained within ± 0.3 mm throughout the density measurements, providing less fluctuations in the temperature data. Furthermore, the molten sample in microgravity waw perfect spheres, which was ideal with regard to calculating the volumes from the sample images. These factors make the ELF a useful apparatus for ascertaining the densities of materials having high melting points, such as refractory oxides, with high accuracy.

Table 3 and Figure 7 summarize the relationship between the Shannon ionic radius and the molar volume at the melting point for Y_2O_3 and other non-glass-forming sesquioxides. The molar volumes shown here were calculated from the densities at the various melting points [11, 14, 15, 19, 20]. The relationship between the ionic radius cubed and the molar volume of each non-glass-forming oxide in Figure 7 shows a strong linear correlation, and the data for the molten Y_2O_3 are consistent with this relationship. These results suggest that the atomic structures of non-glass forming oxides in the liquid state are similar. The liquid atomic structure of Er_2O_3 (one of the non-glass-forming oxides) was previously investigated by Koyama et al. [21]. In this prior work, the structure factor ($S(Q)$) of liquid Er_2O_3 was determined using synchrotron X-ray diffraction in conjunction with an ADL apparatus and the pair distribution function was calculated from the $S(Q)$ and density data acquired using the

TABLE 3
Ionic radius, density and molar volume for various oxides

Oxide metal	**Ionic radius (pm)**	**Density at melting point (kg/m^3)**	**Molar volume at melting point (cm^3/mol)**
Al	53.5	2900	35.2
Ga	62.0	5005	37.5
Lu	86.1	8633	46.1
Yb	86.8	8424	46.8
Tm	88.0	8304	46.5
Er	89.0	8170	46.8
Ho	90.1	8035	47.0
Tb	92.3	7451	49.1
Gd	93.8	7268	49.9
Y	90.0	4690	51.3

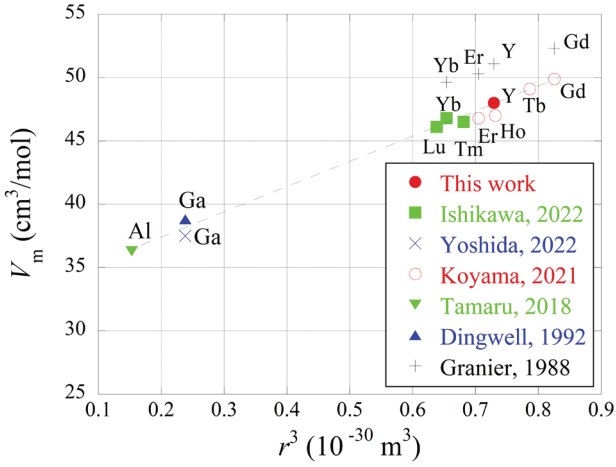

FIGURE 7
The relationship between ionic radius and molar volume for various sesquioxides (A_2O_3).

ISS-ELF. The atomic structure was subsequently constructed using molecular dynamics with reverse Monte Carlo calculations and a persistent homology analysis. The molten material was found to comprise disordered clusters made of OEr_4 tetrahedra that formed a network having a long periodicity. The similar data presented in Figure 7 suggest that the atomic structure of molten Y_2O_3 also involves long periodicity and disordered tetrahedral clusters. Assessments of the atomic structure of Y_2O_3 are currently underway in our laboratory and detailed results will be reported in future publications.

4 CONCLUSION

The density of molten Y_2O_3 was determined using the ELF incorporated in the KIBO module within the ISS. During these trials, Y_2O_3 was successfully levitated and subsequently melted, and the density of this oxide was measured over a wide temperature range. These results confirm that the ELF is able to accurately ascertain the density of refractory materials by providing static conditions without disturbances such as gas jets and by forming perfect spherical samples in microgravity.

ACKNOWLEDGMENTS

The authors are grateful to the ISS crew and the ground operation staff for their support during the onboard experiments. This research is supported by JSPS KAKENHI (Grant No. 20H05882 and 20H05878).

REFERENCES

[1] Chen, Z., Li, Z., Li, J., Liu, C.; Lao, C., Fu, Y., Liu, C., Li, Y., Wang, P., He, Y. 3D printing of ceramics: A review. *J. Eur. Ceram. Soc*.2019, **39**, 661–687.

[2] Ushakov S. V., Niessen, J., Quirinale, D. G., Prieler, R., Navrotsky, A., Telle, R. Measurements of Density of Liquid Oxides with an Aero-Acoustic Levitator, Materials 2021, **14**, 822. https://doi.org/10.3390/ma14040822

[3] Millot, F., Rifflet, J. C., Sarou-Kanian, V., Wille, G., *Int. J. Thermophys.* **23** (2002), 1185–1195, https://doi.org/10.1023/A:1019836102776

[4] Langstaff, D., Gunn, M., Greaves, G. N., Marsing, A., Kargl, F., *Rev. Sci. Instrum.* **84** (2013), 124901, http://dx.doi.org/10.1063/1.4832115

[5] Brillo, J. Egry, I., *J. Mat. Sci.* **40** (2005), 2213–2216, https://doi.org/10.1007/s10853-005-1935-6

[6] Wessing, J. J., Brillo, *J., Met. Mat. Trans*. A **48** (2017), 868–882, https://doi.org/10.1007/s11661-016-3886-8

[7] Richardsen, T. Lohöfer, G., Egry, I., *Int. J. Thermophys.* **23** (2002), 1207–1216, https://doi.org/10.1023/A:1019840203684

[8] Kobatake, H., Fukuyama, H. Tsukada, T., Awaji, S., *Meas. Sci. Technol.* **21**(2010), 025901, https://doi.org/10.1088/0957-0233/21/2/025901

[9] Rhim, W. -K., Chung, S. -K., Barber, D., Man, K. F., Gutt, G., Rulison, A. J., Spujt, R. E., *Rev. Sci. Instrum.* **64** (1993), 2961–2970. https://doi.org/10.1063/1.1144475

[10] Fuse, T., Nakamura, Y., Murakami, K., Shibasaki, K., Tamaru, H., Ohkuma, H., Yukizono, S., Ishikawa, T., Okada, J., Takada, T., Sakai, Y., Arai, T., Fujino, N. *64th International Astronautical Congress Beijing, China* IAC-13-A2.7.8 (2013).

[11] Tamaru, H., Koyama, C., Saruwatari, H., Nakamura, Y., Ishikawa, T., Takada, T. *Microgravity Sci. Technol.***30** (2018), 643–651, https://doi.org/10.1007/s12217-018-9631-8

[12] CRC handbook of chemistry and physics, 81st edition, 2000–2001, CRC Press

[13] Ishikawa, T., Koyama, C., Oda, H., Saruwatari, H., and Paradis, P.-F. (2022a). Status of the electrostatic levitation furnace in the ISS - surface tension and viscosity measurements. *Int. J. Microgravity Sci. Appl.* **39**, 390101. https://doi.org/10.15011/jasma.39.390101

[14] Koyama, C., Ishikawa, T., Oda, H., Saruwatari, H., Ueno, S., Oshio, M., et al. (2021). Densities of liquid lanthanoid sesquioxides measured with the electrostatic levitation furnace in the ISS. *J. Am. Ceram. Soc*. **104**, 2913–2918. https://doi.org/10.1111/jace.17674

[15] Ishikawa, T., Koyama, C., Oda, H., Shimonishi, R., Ito, T., and Paradis, P.-F. (2022b). Densities of liquid Tm_2O_3, Yb_2O_3, and Lu_2O_3 measured by an electrostatic levitation furnace onboard the International Space Station. *Metals* **12**, 1126. https://doi.org/10.3390/met12071126

[16] Chung, S. K.; Thiessen, D. B.; Rhim W.-K. A noncontact measurement technique for the density and thermal expansion coefficient of solid and liquid materials. *Rev. Sci. Instrum.* 1996, **67**, 3175. https://doi.org/10.1063/1.1147584

[17] J. Hlavac, Melting temperature of refractory oxides, *Pure&Appl. Chem.*, vol. 54, No. 3, pp. 681–688 1982.

[18] Granier, B.; Heurtault, S. Density of liquid rare earth sesquioxides. *J. Am. Ceram. Soc.* 1988, 71, C466–C468.

[19] Yoshida, K., Kumagai, H., Yamane, T., Hayashi, A., Koyama, C., Oda, H., Ito, T., Ishikawa, T., Thermophysical properties of molten Ga_2O_3 by using the electrostatic levitation furnace in the International Space Station, *Applied Physics Express* **15**, 085503 (2022), https://doi.org/10.35848/1882-0786/ac7fdd

[20] D. B. Dingwell, *J. Am. Ceram. Soc*. **75**, 1656 (1992).

[21] Koyama, C., Tahara, S., Kohara, S., Onodera, Y., Småbråten, D.R., Selbach, S.M., Akola, J., Ishikawa, T., Masuno, A., Mizuno, A.;et al. Very sharp diffraction peak in liquid Er_2O_3 with crystal-like homology. *NPG Asia Mater*. 2020, 12, 43.